The Rho guanine nucleotide exchange factor ARHGEF5 promotes tumor malignancy via epithelial-mesenchymal transition

(グアニンヌクレオチド交換因子 ARHGEF5 は上皮間葉転換を介するがんの悪性化を促進する)

A Doctoral Thesis

Yu Komiya

Department of Oncogene Research,
Research Institute for Microbial Diseases,
Osaka University

August 2016

Contents

Abbreviations

Arhgef: Rho guanine nucleotide exchange factor (GEF)

Cdc42: Cell division control protein 42 homolog

Cortactin: Cortical actin binding protein

DH domain: Dbl homology domain

FA: Focal adhesion

GAP: GTPase activating proteins

GDP: Guanosine diphosphate

GEF: Guanine nucleotide exchange factor

GTP: Guanosine triphosphate

PH domain: Pleckstrin homology domain

PI3K: Phosphatidyl Isositol 3-kinases

Rac: Ras-related C3 botulinum toxin substrate

SFKs: Src family tyrosine kinases

SH2 domain: Src Homology 2 domain

SH3 domain: Src Homology 3 domain

TIM: Transforming immortalized mammary

General introduction

Cancer

Cancer is a disease of the cells in our body. According to GLOBOCAN 2012, an estimated 14.1 million new cancer cases and 8.2 million cancer-related deaths occurred in 2012. This mortality is caused by cancer invasion or metastasis which unable us to surgical treatment. Cancer is caused by uncontrolled cellular proliferation and most of it is from epithelia. Cancer progression is classified by primary carcinogenesis, invasion which go into stroma by degrading basement membrane and metastasis. Invasion and metastasis significantly decreases prognosis of patient because of treatment difficulty. In 2011, hallmarks of cancer are discussed by Dr. Weinberg, which classified biological characteristics of cancer progression. Hallmarks of cancer comprise 10 biological capabilities acquired during the multistep cancer development; 1 Sustaining proliferative signaling, 2 Evading growth suppressors, 3 Avoiding immune destruction, 4 Enabling replicative immortality, 5 Tumor-promoting inflammation, 6 Activating invasion and metastasis, 7 Inducing angiogenesis, 8 Genome instability and mutation, 9 Resting cell death and 10 Deregulating cellular energetics.

Src-family tyrosine kinases

Src is the first discovered oncogene encodes non receptor tyrosine kinase with high homology between single cell organism Flagellate to mammalian. In mammals, Src family kinases are comprised of 8 members; Src, Yes, Fyn, Lyn, Lck, Hck, Fgr, and Blk. All of Src family kinases share SH2, SH3 and kinase domain. Uncontrolled Src activation causes carcinogenesis or invasiveness in epithelia which are confirmed by lots of experiment both *in*

vitro and *in vivo*. These data promised us that exists of mutation in Src like RAS, however almost no mutation was reported by now ,indicating regulatory mechanism of Src is necessary to be determined.

Epithelial-Mesenchymal Transition

Epithelial cells can convert into mesenchymal cells by a process known as the epithelial–mesenchymal transition (EMT). The term EMT describes a series of events during which epithelial cells lose many of their epithelial characteristics. This phenomena is observed both embryogenesis and during cancer progression. Epithelial cells form layers of cells that are closely adjoined by specialized membrane structures, such as tight junctions, adherens junctions, desmosomes and gap junctions. Mesenchymal cells, on the other hand, do not form an organized cell layer, nor do they have the same apical–basolateral organization and polarization of the cell surface molecules and the actin cytoskeleton as epithelial cells. In culture *in vitro*, mesenchymal cells have a spindle-shaped, whereas epithelial cells grow as clusters of cells that maintain complete cell–cell adhesion with their neighbors. Since 1980, a number of molecular differences have been observed between mesenchymal and epithelial cells. For example, epithelial cells express E-cadherin, Occludin and Cytokeratin and mesenchymal cells express N-cadherin, Vimentin and Fibronectin and these are used as EMT markers to determine the epithelial or mesenchymal status.

Abstract

Epithelial tumor cells often acquire malignant properties, such as invasion/metastasis and uncontrolled cell growth, by undergoing epithelial-mesenchymal transition (EMT). However, the mechanisms by which EMT contributes to malignant progression remain elusive. Here, I show that the Rho guanine nucleotide exchange factor (GEF) ARHGEF5 promotes tumor

malignancy in a manner dependent on EMT status. We previously identified ARHGEF5, a member of the Dbl family of GEFs, as a multifunctional mediator of Src-induced cell invasion and tumor growth. In the present study, ARHGEF5 was upregulated during TGF-β-induced EMT in human epithelial MCF10A cells, and promoted cell migration by activating the Rho-ROCK pathway. ARHGEF5 was necessary for the invasive and in vivo metastatic activity of human colorectal cancer HCT116 cells. These findings underscore the crucial role of ARHGEF5 in cell migration and invasion/metastasis. An in vivo tumorigenesis assay revealed that ARHGEF5 had the potential to promote tumor growth via the PI3K pathway. However, ARHGEF5 was not required for tumor growth in epithelial-like human colorectal cancer HCT116 and HT29 cells, whereas the growth of mesenchymal-like SW480 and SW620 cells depended on ARHGEF5. Induction of EMT by TNF-α or Slug in HCT116 cells resulted in the dependence of tumor growth on ARHGEF5. In these mesenchymal-like cells, Akt was activated via ARHGEF5 and its activity was required for tumor growth. Aanalysis of a transcriptome dataset revealed that the combination of ARHGEF5 upregulation and E-cadherin downregulation or Snail upregulation was significantly correlated with poor prognosis in patients with colorectal

cancers. Taken together, our findings suggest that EMT-induced ARHGEF5 activation contributes to the progression of tumor malignancy. ARHGEF5 may serve as a potential therapeutic target in a subset of malignant tumors that have undergone EMT.

Introduction

The malignant progression of tumor cells is associated with acquisition of invasive and metastatic properties and uncontrolled cell growth[1, 2]. Over the course of this process, epithelial tumor cells often undergo epithelial-mesenchymal transition (EMT)[3-6], a reversible phenotypic change that takes place during embryonic development, wound-healing, and malignant progression. EMT is generally characterized by the downregulation of epithelial markers such as E-cadherin and occludin, and the upregulation of mesenchymal markers such as N-cadherin, vimentin and matrix metalloproteinases (MMPs). During EMT, epithelial cells lose cell-cell junctions and apico-basal polarity, and acquire invasive phenotypes that are essential for metastatic spread. These directional shifts in gene expression are regulated by several transcription factors, including Snail, Slug, and ZEB1/2; these are induced by cell signaling activated by cytokines and growth factors such as TGF-β[7], TNF-α[8, 9], EGF[10], and HGF[10]. Mutations and/or epigenetic alterations in these EMT driver genes play a role in EMT induction[11, 12], and they correlate with disease relapse and survival in patients with cancer. These observations indicate that an aberrant EMT process leads to poor clinical outcomes[13, 14]. Furthermore, suppression of EMT can increase sensitivity to anti-cancer drugs[15, 16]. Therefore, the identification of EMT characteristics and inhibitors of EMT-related

molecules could potentially contribute to the treatment of cancer. The invasive and metastatic potential of tumor cells is partly regulated by the Src family of non-receptor tyrosine kinases[17]. Src is upregulated in various human cancers, resulting in the deregulated turnover of focal adhesions and cytoskeletal remodeling, thereby

promoting cell adhesion and migration[18, 19]. Src also contributes to tumor invasion by inducing the expression of MMPs via the STAT3 pathway[20]. In a previous study, we dissected Src signaling using an inducible system for Src activation[21] and found that the Rho guanine nucleotide exchange factor (GEF) ARHGEF5, a member of the Dbl family of Rho GEFs, is crucial for Src-induced formation of podosomes (or invadopodia)[21]. Podosomes are protruding

membrane structures with the ability to degrade the extracellular matrix (ECM), and their formation is tightly associated with the invasive potential of tumor cells[22, 23]. Furthermore, we showed that ARHGEF5 is phosphorylated by Src, resulting in the elevation of GEF activity toward RhoA[21, 24]. These results suggest that ARHGEF5 mediates the Src oncogenic signal to promote invasive potential via the Rho pathway[25]. ARHGEF5 is induced by Smad signals during TGF-β-induced mesenchymal transition of endothelial cells (EndMT)[26], suggesting a role for ARHGEF5 in the TGF-β-induced cytoskeletal remodeling. Furthermore, ARHGEF5 was identified as an important factor in the chemotaxis of macrophage-related cells by siRNA

screening[27]. Despite functional compensation by related GEFs, ARHGEF5 null mice exhibited an impaired chemotaxis of immature dendritic cells (DCs) and reduced migration of DCs from the skin to the lymph nodes[27].

Taken together, these observations highlight the crucial role of ARHGEF5 in regulating cytoskeletal remodeling linked to cell migration and invasion. The ARHGEF5 gene was originally identified as an oncogene by focus formation assays in NIH3T3 cells[28, 29]. Recent reports showed that ARHGEF5 upregulation promotes tumorigenesis[30], and that co-expression of ARHGEF5 and Src is associated with poor prognosis of patients with non-small cell lung cancer[31]. In addition, ARHGEF5 overexpression dramatically increase Src-induced tumor growth[21], implying that the Src-ARHGEF5 pathway plays important roles not only in invasion and metastasis, but also in tumor growth. However, the function and regulation of this pathway during malignant progression remain elusive. In the present study, I focused our analysis on the function of ARHGEF5 in the context of EMT because of its potential link to malignant progression. I show that ARHGEF5 is functionally upregulated during EMT and promotes invasion/metastasis and tumor growth, particularly in cells that have acquired mesenchymal phenotypes. In support of this, analysis of a transcriptome dataset revealed that the combination of ARHGEF5 upregulation and E-cadherin downregulation or Snail upregulation is significantly correlated with poor prognosis in patients with colorectal cancers. These findings indicate that EMT-induced ARHGEF5

activation contributes to the progression of tumor malignancy. ARHGEF5 may serve as a potential therapeutic target of a subset of malignant tumors that have undergone EMT.

Results

Arhgef5 and Src are upregulated during TGF-ß-induced EMT in MCF10A

cells.

To determine the relevance of ARHGEF5 to EMT, the effects of TGF-β-induced EMT on the expression and function of ARHGEF5 were examined using the human breast epithelial MCF10A cell line as a model system. TGF-β treatment induced apparent morphological changes in MCF10A cells, which were accompanied by E-cadherin downregulation, N-cadherin upregulation, actin cytoskeleton rearrangement, and the formation of podosome-like structures (Figure 1A and B). In addition, TGF-β treatment strongly promoted cell migration (Figure 1C). These observations confirmed that TGF-β induced EMT in these cells. These processes were accompanied by ARHGEF5 upregulation at the protein and mRNA levels (Figure 2A and B). Since TGF-β signaling is basally activated in MCF10A cells via the autocrine action of TGF-β[32], blockade of TGF-β signaling with the TGF-β receptor inhibitor SD208 downregulated ARHGEF5 expression (Figure 2C). The phosphorylation of myosin light chain (MLC) was altered in parallel with ARHGEF5 expression levels in response to treatment with TGF-β and SD208 (Figure 2A and C), indicating that ARHGEF5 is involved in the activation of the Rho-ROCK pathway[25]. To examine the functional link between ARHGEF5 and Src, we investigated the expression and function of Src family kinases during TGF-β-induced EMT. The expression and activity (pY418 signals) of Src and Fyn, which function at focal adhesions[17], were elevated during EMT, concomitant with increased phosphorylation of their substrates, cortactin and

focal adhesion kinase (FAK) (Figure 2D). Induction of EMT resulted in the accumulation of ARHGEF5 in regions near the edges of lamellipodia, where focal adhesion molecules, including tyrosine phosphorylated proteins and

actin fibers, are directed (Figure 2E)[33]. These findings demonstrate that ARHGEF5 and Src are upregulated and accumulate at sites of cell adhesion during TGF-β-induced EMT.

ARHGEF5 knockdown attenuates TGF-β-induced EMT phenotypes and cell migration in MCF10A cells

To verify the contribution of ARHGEF5 to EMT, we examined the effects of ARHGEF5 knockdown (KD) on cell morphology and motility. ARHGEF5 KD suppressed EMT-induced MLC phosphorylation and MLC protein levels (Figure 3A). Immunofluorescence analyses revealed that ARHGEF5 KD attenuated N-cadherin membrane presentation and loss of E-cadherin-mediated cell-cell contacts (Figure 3B). Wound-healing assays revealed that ARHGEF5 KD suppressed cell migration in TGF-β-treated MCF10A cells, whereas it did not significantly affect cell migration in untreated cells (Figure 3C and D). Similar suppressive effects on TGF-β-induced EMT phenotypes were observed in response to ROCK inhibition by Y27632 (Figure 4A-C). Furthermore, ARHGEF5 overexpression induced hyper-phosphorylation of MLC, but was neutralized by treatment with Y27632 (Figure 4D). These results suggest that ARHGEF5 is involved in the progression of EMT phenotypes via activation of the Rho-ROCK pathway. However, ARHGEF5 KD did not affect the TGF-β-mediated induction of EMT-related transcription factors, including SNAI1/2/3, TWIST1/2, and ZEB1/2 (Figure 5), suggesting that ARHGEF5 functions downstream of these transcription factors in the TGF-β signaling pathway.

ARHGEF5 promotes cell migration and invasion in colorectal cancer cells

To evaluate the role of ARHGEF5 in human cancer cells, we examined the effects of ARHGEF5 KD on invasion and metastasis in human colorectal

cancer HCT116 cells with invasive and metastatic activity. Immunofluorescence analysis showed that ARHGEF5 KD induced a rearrangement of the actin cytoskeleton (Figure 6A). Wound-healing and Transwell invasion assays revealed that ARHGEF5 KD significantly impaired cell migration (Figure 6B) and invasion (Figure 6C), respectively. Furthermore, In experimental metastasis assays in nude mice, control HCT116 cells formed metastatic lesions in the lungs of five out of six mice, while ARHGEF5 KD cells did not metastasize to the lungs in any of the mice examined (Figure6D). These findings suggest that ARHGEF5 is involved in the invasive and metastatic activity of some human cancers.

ARHGEF5 promotes tumor growth in mesenchymal-like cancer cells

We previously showed that ARHGEF5 promotes anchorage-independent cell growth of Src-activated fibroblasts (NIH3T3-Src-MER cells)[21]. Xenograft assays in nude mice revealed that the expression of wild-type ARHGEF5 greatly promoted tumorigenesis in Src-activated fibroblasts, whereas mutant ARHGEF5 lacking GEF activity (ΔDH) or Src/PI3K binding domain (Δ583-902) had no effect (data not shown). These observations suggest that ARHGEF5 has the potential to promote tumor growth via the Rho-ROCK and PI3K-Akt pathways. To elucidate the role of ARHGEF5 in tumor growth from human colorectal cancer cells, I examined the effects of ARHGEF5 KD on anchorage-independent cell growth in epithelial-like HCT116 and HT29 cells as well as in mesenchymal-like SW480 and SW620 cells (Figure 7A and B). These cell types were categorized based on the expression of E-cadherin and vimentin (Figure 7A). The effects varied depending on cell type: ARHGEF5 KD did not affect the growth of epithelial-like HCT116 and HT29 cells (Figure 7C), but significantly suppressed the growth of

mesenchymal-like SW480 and SW620 cells (Figure 7D). ARHGEF5 KD also suppressed in vivo tumorigenesis of SW480 cells (Figure 7E). These findings demonstrate that ARHGEF5 contributes to tumor growth, particularly in mesenchymal-like cancer cells, suggesting that the tumorigenic function of ARHGEF5 may be dependent on EMT status. To explore this possibility, EMT was induced in epithelial-like HCT116 cells. Although TGF-β failed to induce EMT in these cells, TNF-α did, as determined by changes in cell morphology and the expression of N-canherin, vimentin, and E-cadherin (Figure 8A). ARHGEF5 KD in TNF-α-treated cells potently suppressed anchorage-independent cell growth (Figure 8B). Furthermore, we forcedly induced EMT in these cells by overexpressing the pro-EMT transcription factor Slug[34](Figure 8C). Slug-induced EMT also sensitized these cells to growth suppression by ARHGEF5 KD (Figure 8D). These observations suggest that the tumorigenic functions of ARHGEF5 are activated when cancer cells acquire mesenchymal phenotypes via EMT.

ARHGEF5-dependent activation of Akt is required for tumor growth in mesenchymal-like colorectal cancer cells

I then addressed the molecular mechanisms underlying the ARHGEF5-dependent tumor growth from mesenchymal-like cancer cells. Previously, we showed that ARHGEF5 interacts with phosphatidylinositol 3-kinase (PI3K)[21], implicating ARHGEF5 in the regulation of the Akt pathway, which is tightly associated with tumor growth. We therefore investigated the impact of EMT status on the activity of Akt in HCT116 cells. During TNF-α-induced EMT, Akt was gradually activated in parallel with the induction of N-cadherin, and ARHGEF5 KD suppressed Akt activation (Figure 9A). Akt was in an active state in mesenchymal-like SW480 and

SW620 cells, but not in epithelial-like HT29 cells, and ARHGEF5 KD attenuated Akt activation in mesenchymal-like cells (Figure 9B). Furthermore, the inhibition of Akt activity by the Akt
inhibitor triciribine significantly suppressed the anchorage-independent growth of these cells (Figure 9C). These results suggest that Akt is activated via ARHGEF5 specifically in cells that have acquired mesenchymal phenotypes, thereby triggering cell signaling required for the promotion of tumor growth.

ARHGEF5 upregulation associated with EMT-related gene expression is correlated with poor prognosis in patients with colorectal cancers

To ascertain the relevance of ARHGEF5 in cancer patients, we examined the correlation between ARHGEF5 expression and prognosis in patients with colorectal cancers. To this end, we analyzed the transcriptome dataset of colorectal cancer provided by The Cancer Genome Atlas (TCGA) project[35]. Given the functional link between ARHGEF5 and EMT in our in vitro observations, we also investigated the expression of E-cadherin (CDH1) and Snail (SNAI1) to stratify the patients. In this study, patients with gene expression levels in upper 60% (ARHGEF5 and SNAI1) were defined as the "High" group and those in lower 60% (CDH1) as the "Low" group, whereas the remaining patients were designated as "Others". The ARHGEF5-High group showed a slight tendency towards a poorer prognosis than the Others, although the difference was not significant (Figure 10A). Similarly, the CDH1-Low group showed a tendency towards a poorer prognosis than the Others, although the difference was not statistically significant. However, in a combined analysis, the ARHGEF5-High/CDH1-Low (HL) group had a significantly worse prognosis than the Others. On the other hand, the

SNAI1-High group by itself had a significantly poorer prognosis than the Others (Figure 10B). Combined analysis of ARHGEF5 and SNAI1 revealed that the prognosis of the ARHGEF5-High/SNAI1-High (HH) group was markedly worse than that of the Others. Furthermore, the ARHGEF5-High/CDH1-Low/SNAI1-High (HLH) group showed the best separation from the Others and the most significant statistical difference (Figure 10C). These data are consistent with the notion that EMT status correlate with the prognosis of colorectal cancers, and support our findings that increased activation of ARHGEF5 contributes to the progression of tumor malignancy in a manner dependent on EMT status.

Discussion

Here, we showed that ARHGEF5 plays a pivotal role in malignant progression, namely the acquisition of invasive/metastatic properties and promotion of tumor growth, particularly in colorectal cancer cells that gained mesenchymal phenotypes via EMT. EMT is a crucial step in malignant progression as it involves the loss of cell polarity, detachment from the epithelial layer, migration, and invasion. Dynamic cytoskeletal remodeling regulated by Rho GTPases is thought to be responsible for these processes[36]; however, regulation of Rho GTPases activity during EMT remains unclear. We found that ARHGEF5 is upregulated during TGF-β-induced EMT and is required for activation of the RhoA-ROCK pathway. A previous study showed that ARHGEF5 expression is induced by Smad signals during TGF-β-induced mesenchymal transition in MS-1 endothelial cells (EndMT)[26]. Thus, expression of ARHGEF5 may be commonly regulated during EMT and EndMT through the TGF-β-Smad pathway. In the present study, Src and Fyn

tyrosine kinases were upregulated during EMT in parallel with ARHGEF5 upregulation. Previous studies show that ARHGEF5 is phosphorylated by Src,

causing a conformational change that leads to increased GEF activity toward RhoA[21, 24]. Therefore, it is likely that Src/Fyn upregulation synergistically potentiates the activity of ARHGEF5, thereby promoting EMT via the Rho-ROCK pathway[25]. The formation of podosomes/invadopodia has been implicated in the invasive and metastatic potential of cancer cells[22, 23, 37]. Src activity is necessary for podosome formation, and active Rho, which localizes to podosomes, is required for the assembly of these structures[38]. We identified ARHGEF5 as a GEF responsible for the activation of podosomal Rho[21], and an extended analysis using ARHGEF5 KO MEFs corroborated that ARHGEF5 accumulates in podosomes and is essential for Src-induced podosome formation (data not shown). Thus, the EMT-mediated upregulation of the Src-ARHGEF5-Rho axis may contribute to the acquisition of invasive and metastatic properties by promoting podosome/invadopodia formation.

The present study showed that ARHGEF5 is crucial for tumor growth, particularly in mesenchymal-like cells. ARHGEF5 KD inhibited tumor growth from mesenchymal-like colorectal cancer SW480 and SW620 cells, while it failed to suppress the growth of epithelial-like HCT116 and HT29 cells. These observations suggest that the acquisition of mesenchymal phenotypes is required for the tumorigenic function of ARHGEF5. In support of this notion, forcedly induction of EMT in HCT116cells sensitized these cells to growth suppression by ARHGEF5 KD. Mesenchymal cells generated by EMT form cell adhesion sites, i.e., focal adhesions and/or

podosomes/invadopodia, at which the Src-ARHGEF5-Rho axis is upregulated and activated21. Since ARHGEF5 can also function as a scaffold for PI3K[21], upregulated ARHGEF5 may activate Akt pathways, thereby promoting cell survival via the anti-apoptotic pathway and cell growth via the mTORC1 pathway[39]. Indeed, we observed that ARHGEF5-dependent activation of Akt was required for tumor growth from mesenchymeal-like colorectal cancer cells. These results suggest that the EMT-mediated assembly of the ARHGEF5 axis at cell adhesion sites plays a crucial role in promoting both cell invasion/metastasis and umor growth in mesenchymal-like cancer cells (Figure 11). To extend the EMT-dependent function of ARHGEF5 to human cancer patients, we investigated the correlation between ARHGEF5/EMT markers and prognosis in patients with colorectal cancers. Although ARHGEF5 expression alone did not correlate significantly with poor prognosis, patients with high ARHGEF5 expression in the CDH1-Low group had a remarkably poorer prognosis than the other patients. Likewise, the ARHGEF5-High/SNAI1-High group had a much poorer prognosis than the other patients. Notably, the ARHGEF5-High/CDH1-Low/SNAI1-High group had the worst prognosis in all settings. These findings support the idea that the functions of ARHGEF5 depend on EMT status, even in human colorectal cancers. In pancreatic cancers, however, the single ARHGEF5-High group had a significantly poorer prognosis than the Others (Figure 10D), supporting the important role of ARHGEF5 in this tumor type. On the other hand, there was no significant correlation between ARHGEF5/EMT and prognosis in breast cancers that typically invade as an epithelial multicellular unit[40] (data not shown). These findings suggest that, although the contribution of ARHGEF5/EMT varies depending on tumor types and

their strategies for invasion and metastasis, ARHGEF5 and related molecules may represent

potential targets for the treatment of a subset of malignant tumors that have undergone EMT.

Fig. 1

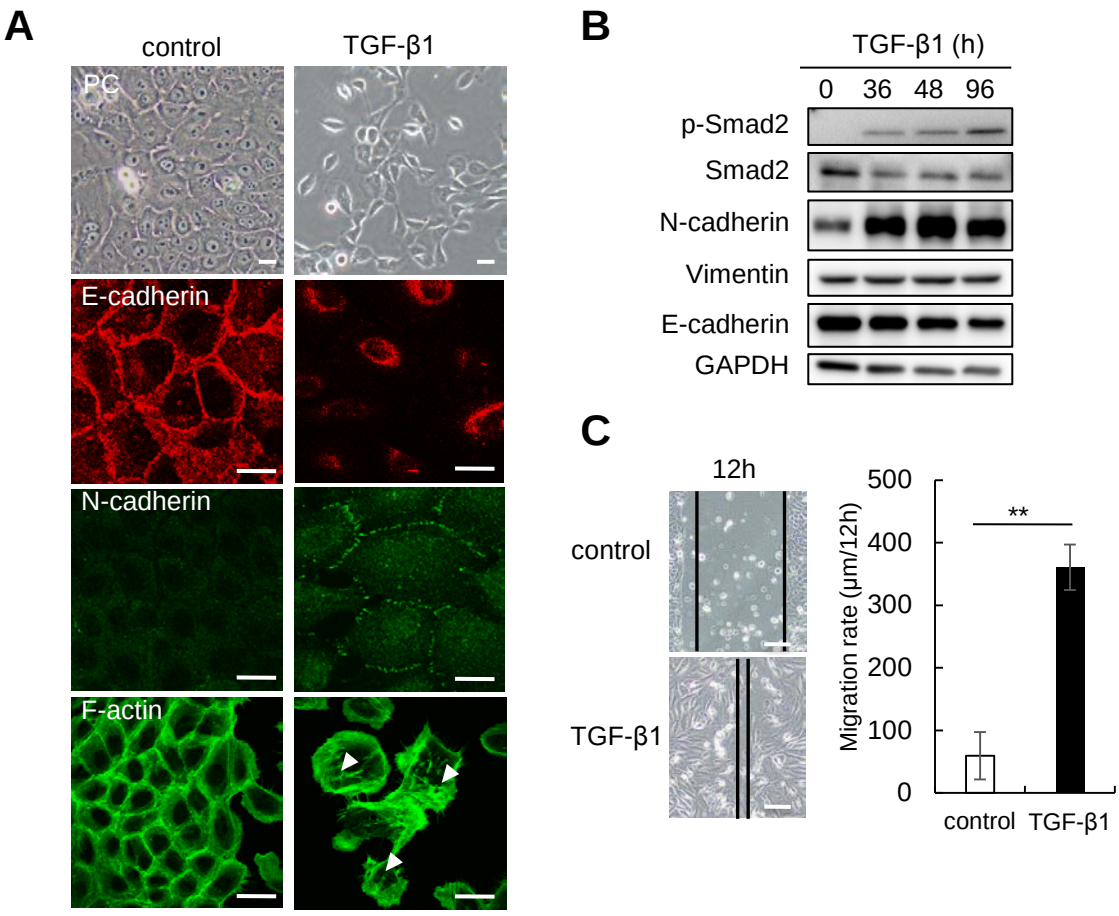
A
control
TGF-β1
PC
E-cadherin
N-cadherin
F-actin
B
TGF-β1 (h)
0
36
48
96
p-Smad2
Smad2
N-cadherin
Vimentin
E-cadherin
GAPDH
C
12h
control
TGF-β1
Migration rate (μm/12h)
500
400
300
200
100
0
**
control
TGF-β1

Fig. 2

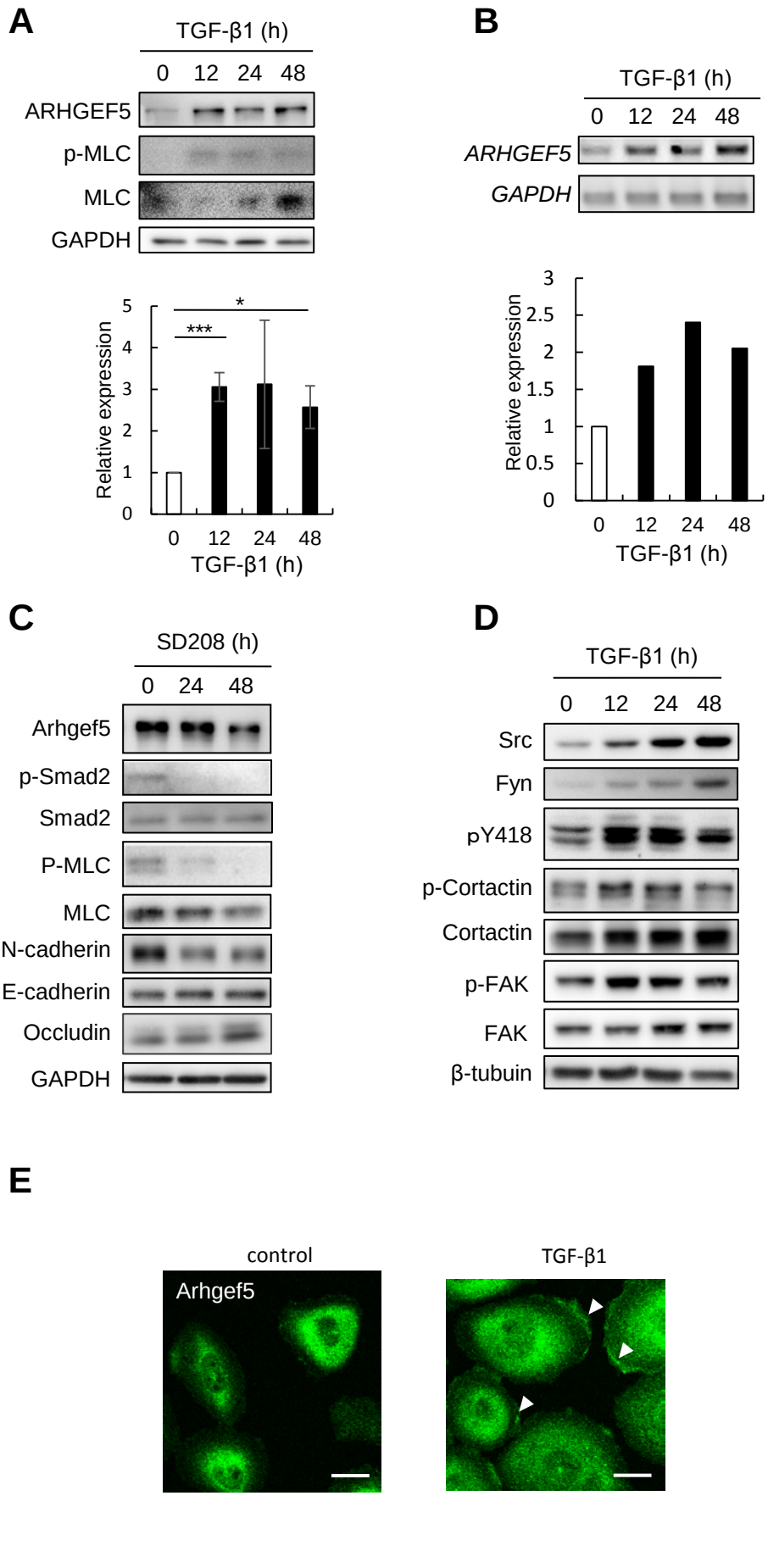
A
TGF-β1 (h)
0 12 24 48
ARHGEF5
p-MLC
MLC
GAPDH
Relative expression
0 1 2 3 4 5
*
***
0 12 24 48
TGF-β1 (h)
B
TGF-β1 (h)
0 12 24 48
ARHGEF5
GAPDH
Relative expression
0 0.5 1 1.5 2 2.5 3
0 12 24 48
TGF-β1 (h)
C
SD208 (h)
0 24 48
Arhgef5
p-Smad2
Smad2
P-MLC
MLC
N-cadherin
E-cadherin
Occludin
GAPDH
D
TGF-β1 (h)
0 12 24 48
Src
Fyn
pY418
p-Cortactin
Cortactin
p-FAK
FAK
β-tubuin
E
control
TGF-β1
Arhgef5

Fig. 3

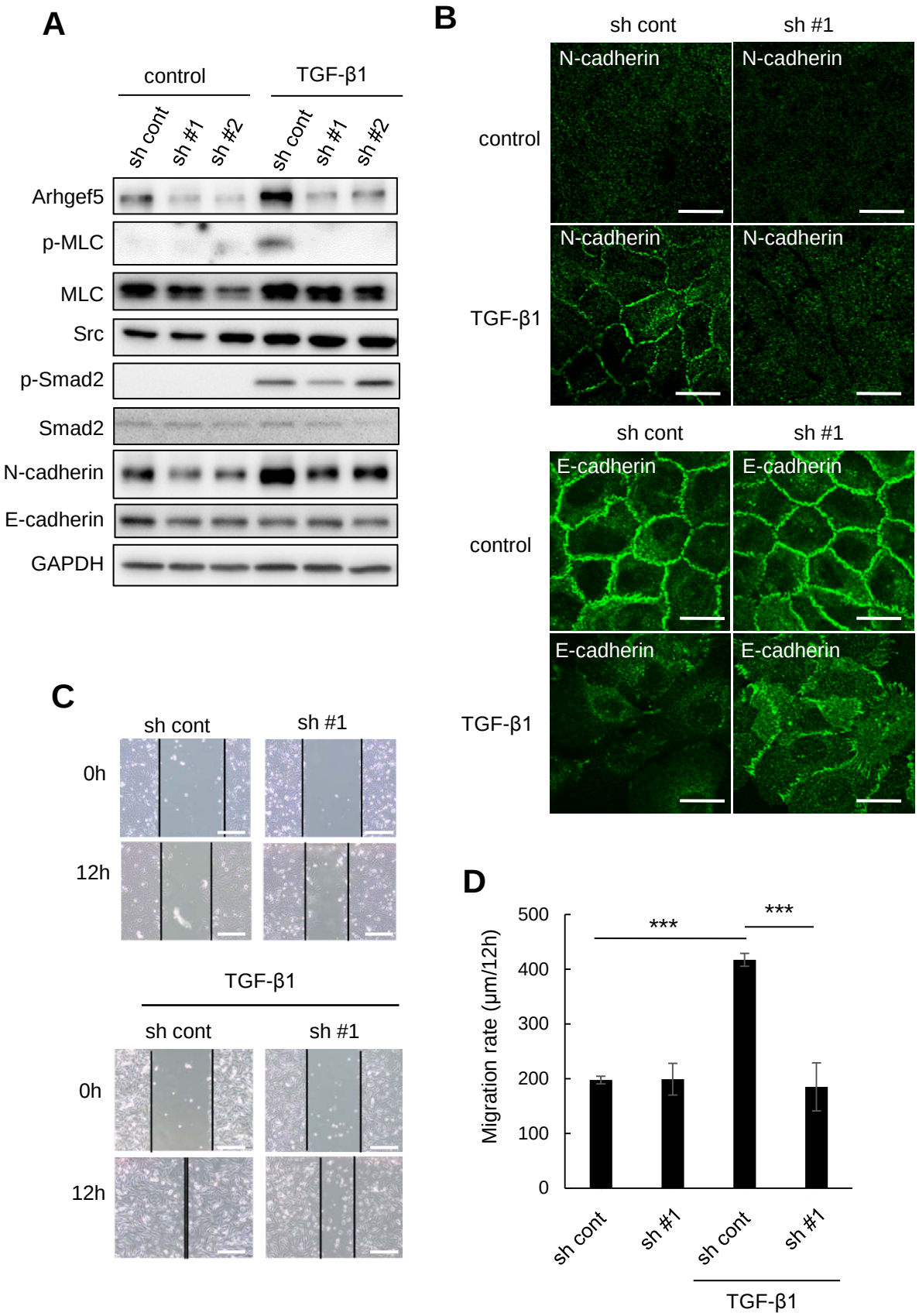
A
control
TGF-β1
sh cont
sh #1
sh #2
sh cont
sh #1
sh #2
Arhgef5
p-MLC
MLC
Src
p-Smad2
Smad2
N-cadherin
E-cadherin
GAPDH
B
sh cont
sh #1
N-cadherin
N-cadherin
control
N-cadherin
N-cadherin
TGF-β1
sh cont
sh #1
E-cadherin
E-cadherin
control
E-cadherin
E-cadherin
TGF-β1
C
sh cont
sh #1
0h
12h
TGF-β1
sh cont
sh #1
0h
12h
D
Migration rate (μm/12h)
500
400
300
200
100
0
***
***
sh cont
sh #1
sh cont
sh #1
TGF-β1

Fig. 4

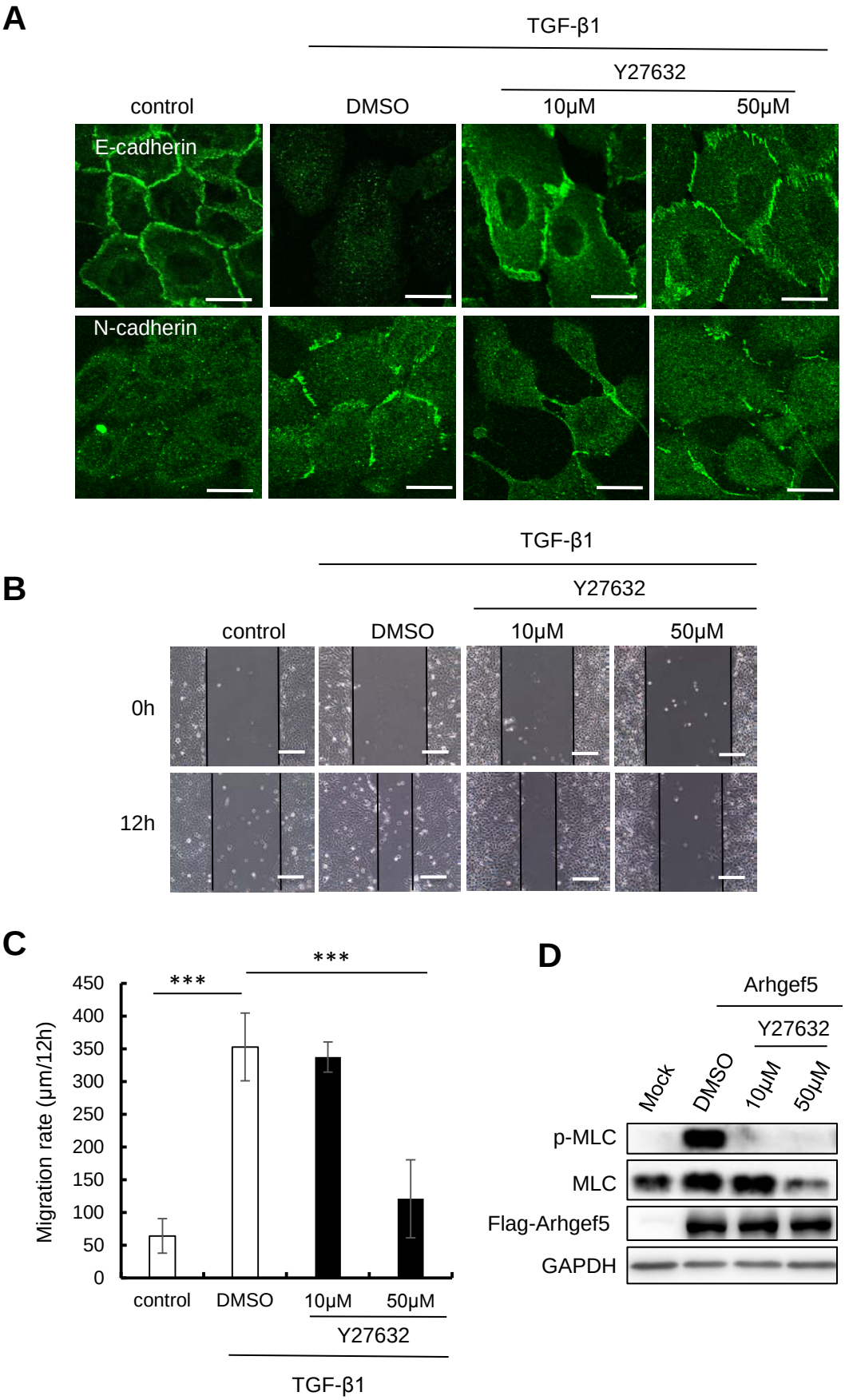
A
TGF-β1
Y27632
control
DMSO
10μM
50μM
E-cadherin
N-cadherin
B
TGF-β1
Y27632
control
DMSO
10μM
50μM
0h
12h
C
***
***
Migration rate (μm/12h)
450
400
350
300
250
200
150
100
50
0
control
DMSO
10μM
50μM
Y27632
TGF-β1
D
Arhgef5
Y27632
Mock
DMSO
10μM
50μM
p-MLC
MLC
Flag-Arhgef5
GAPDH

Fig. 5

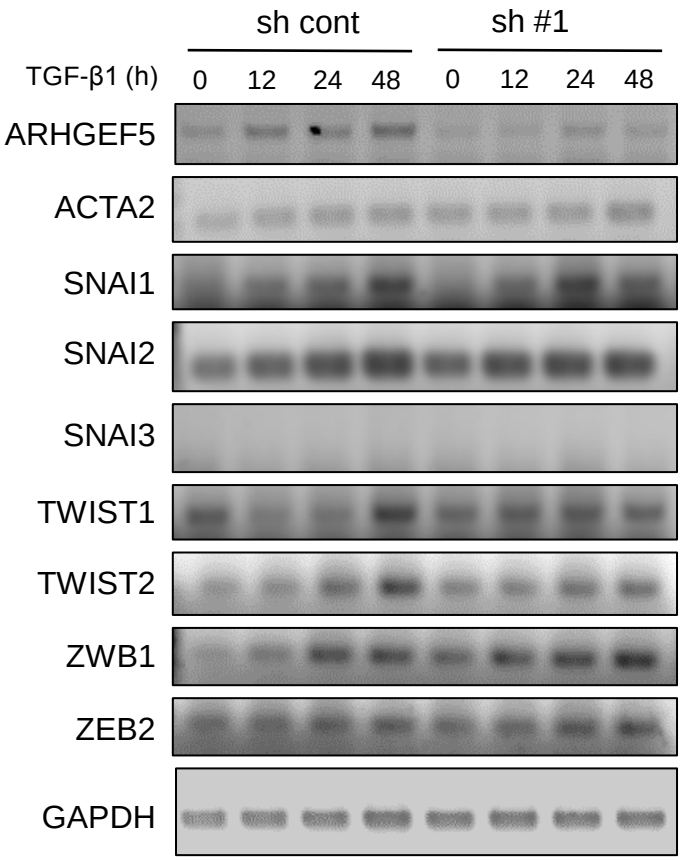
sh cont
sh #1
TGF-β1 (h)
0
12
24
48
0
12
24
48
ARHGEF5
ACTA2
SNAI1
SNAI2
SNAI3
TWIST1
TWIST2
ZWB1
ZEB2
GAPDH

Fig. 6

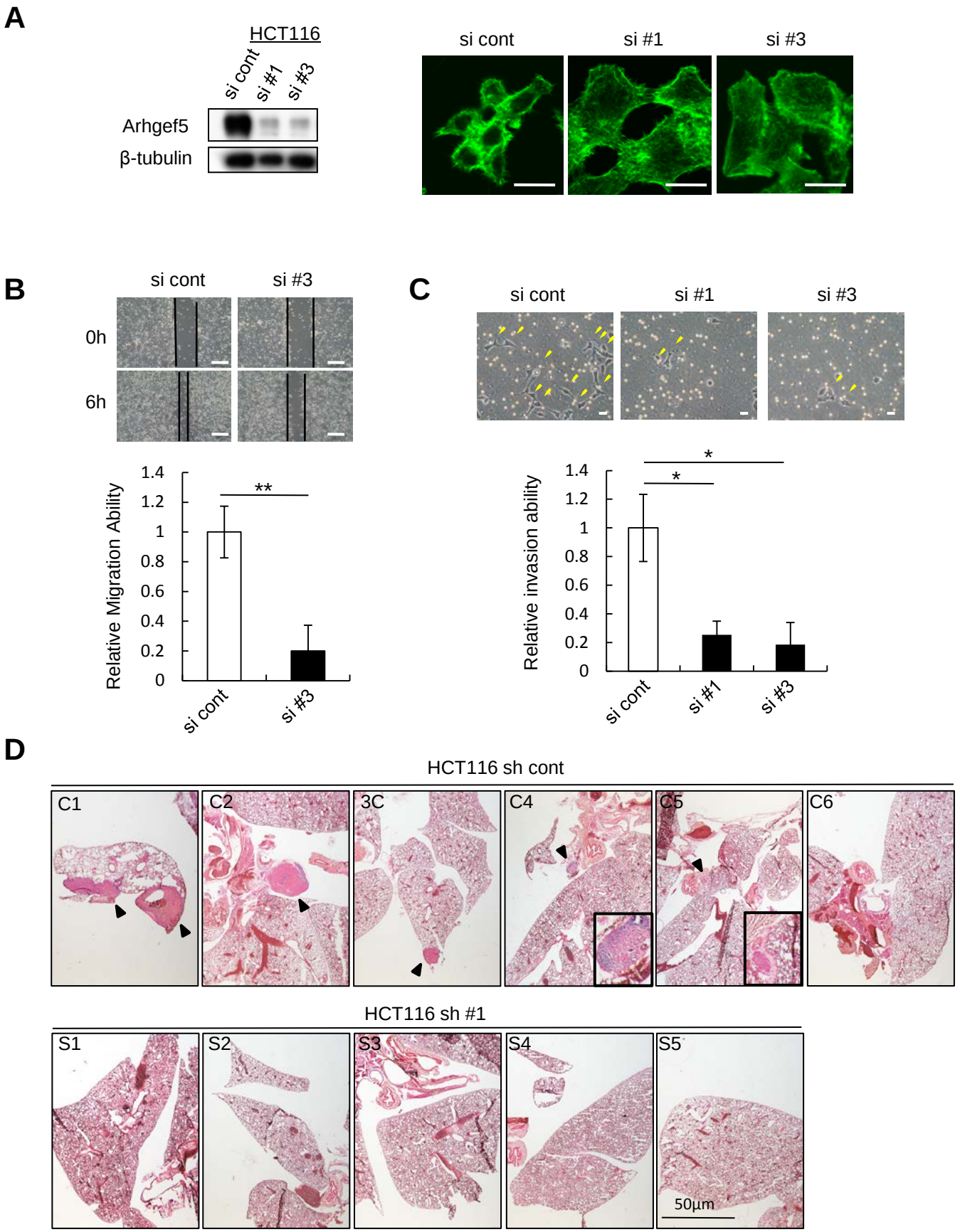
A
HCT116
si cont
si #1
si #3
Arhgef5
β-tubulin
si cont
si #1
si #3
B
si cont
si #3
0h
6h
Relative Migration Ability
1.4
1.2
1
0.8
0.6
0.4
0.2
0
**
si cont
si #3
C
si cont
si #1
si #3
Relative invasion ability
1.4
1.2
1
0.8
0.6
0.4
0.2
0
*
*
si cont
si #1
si #3
D
HCT116 sh cont
C1
C2
3C
C4
C5
C6
HCT116 sh #1
S1
S2
S3
S4
S5
50μm

Fig. 7

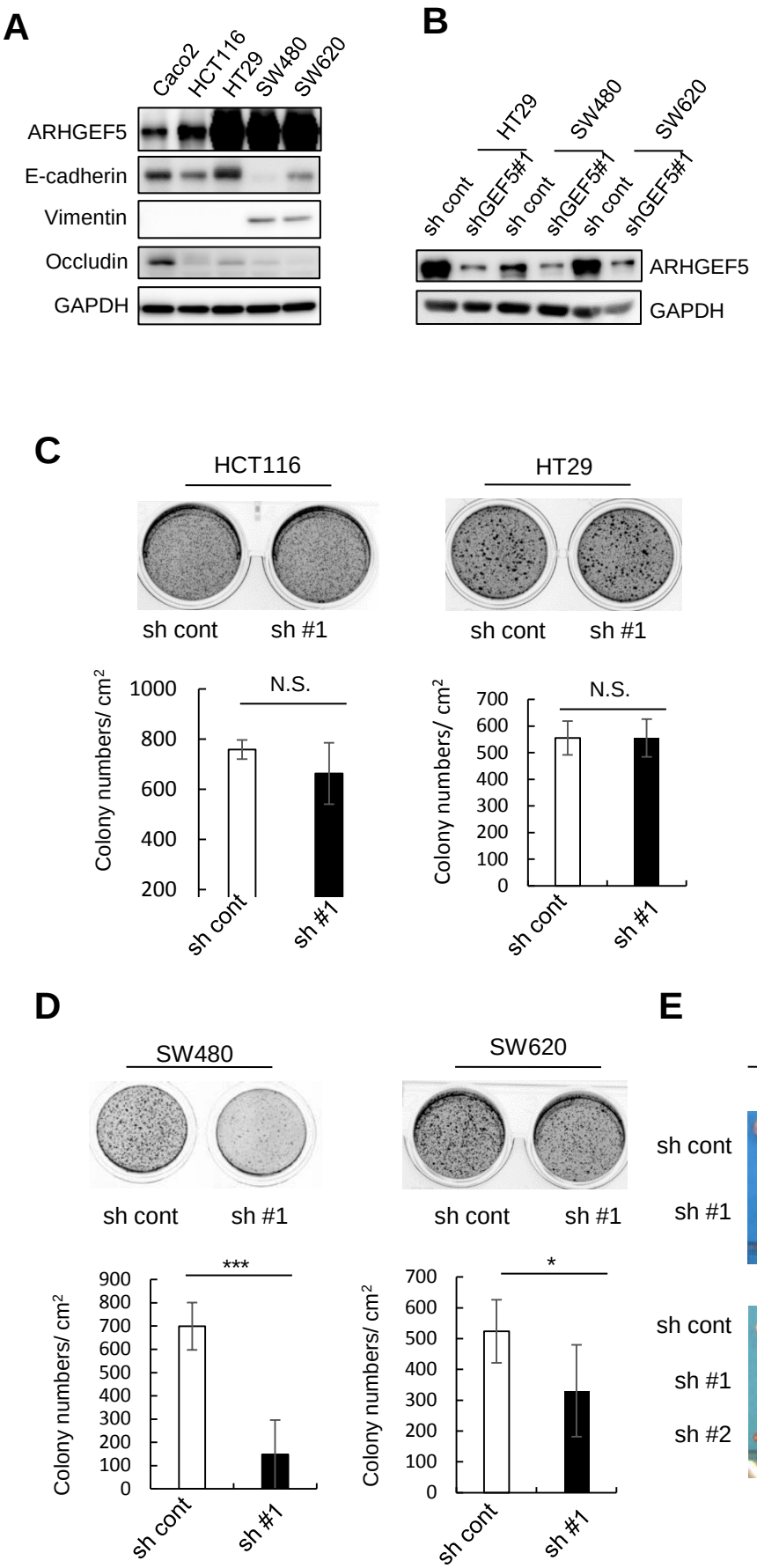
A
Caco2
HCT116
HT29
SW480
SW620
ARHGEF5
E-cadherin
Vimentin
Occludin
GAPDH
B
HT29
SW480
SW620
sh cont
shGEF5#1
sh cont
shGEF5#1
sh cont
shGEF5#1
ARHGEF5
GAPDH
C
HCT116
HT29
sh cont
sh #1
sh cont
sh #1
Colony numbers/ cm2
N.S.
1000
800
600
400
200
sh cont
sh #1
Colony numbers/ cm2
N.S.
700
600
500
400
300
200
100
0
sh cont
sh #1
D
SW480
SW620
sh cont
sh #1
sh cont
sh #1
Colony numbers/ cm2
***
900
800
700
600
500
400
300
200
100
0
sh cont
sh #1
Colony numbers/ cm2
*
700
600
500
400
300
200
100
0
sh cont
sh #1
E
SW480
Exp.1 (n=4)
sh cont
sh #1
Exp.2 (n=3)
sh cont
sh #1
sh #2

Fig. 8

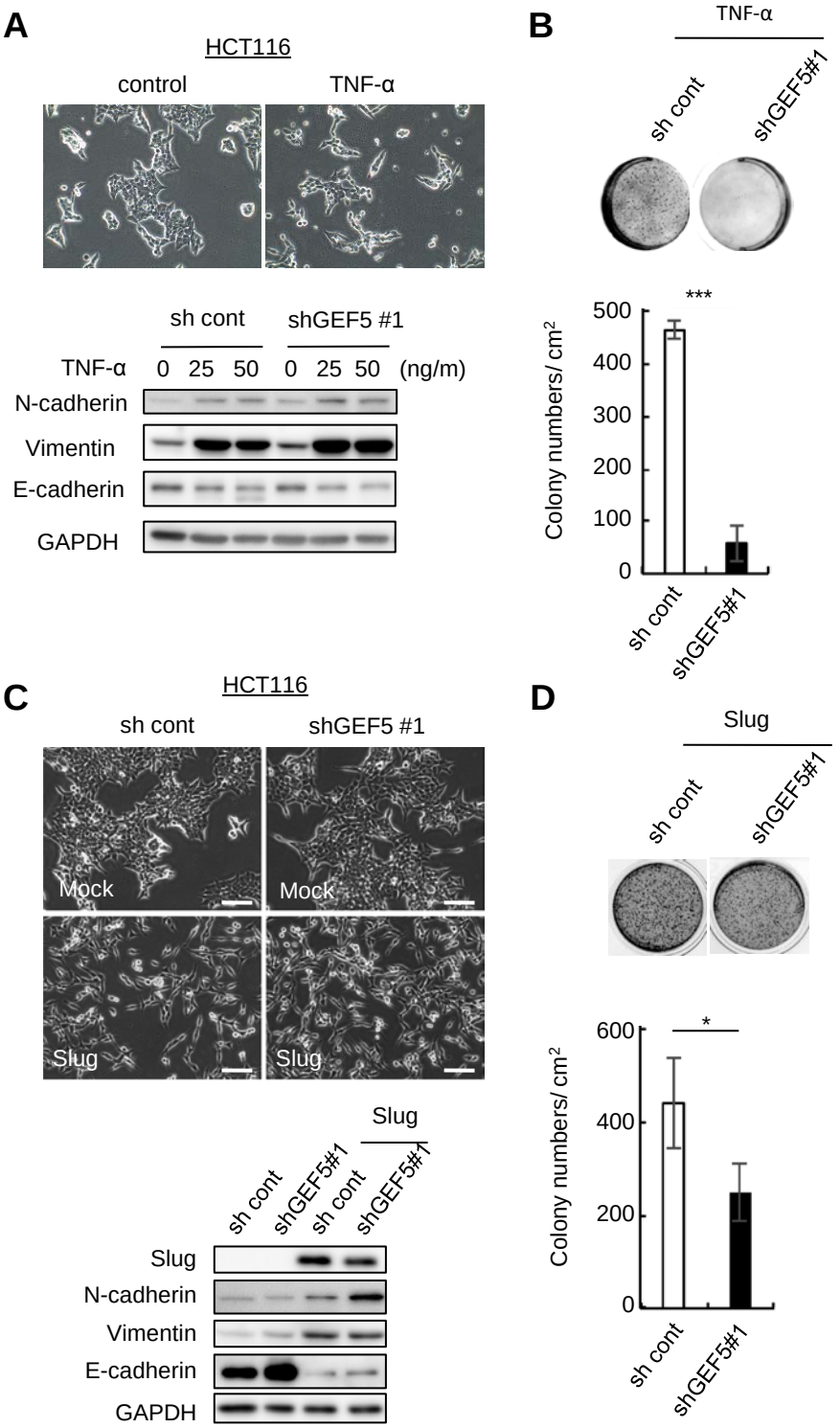
A
HCT116
control
TNF-α
sh cont
shGEF5 #1
TNF-α 0 25 50 0 25 50 (ng/m)
N-cadherin
Vimentin
E-cadherin
GAPDH
B
TNF-α
sh cont
shGEF5#1
***
Colony numbers/ cm2
500
400
300
200
100
0
sh cont
shGEF5#1
C
HCT116
sh cont
shGEF5 #1
Mock
Mock
Slug
Slug
Slug
sh cont
shGEF5#1
sh cont
shGEF5#1
Slug
N-cadherin
Vimentin
E-cadherin
GAPDH
D
Slug
sh cont
shGEF5#1
*
Colony numbers/ cm2
600
400
200
0
sh cont
shGEF5#1

Fig. 9

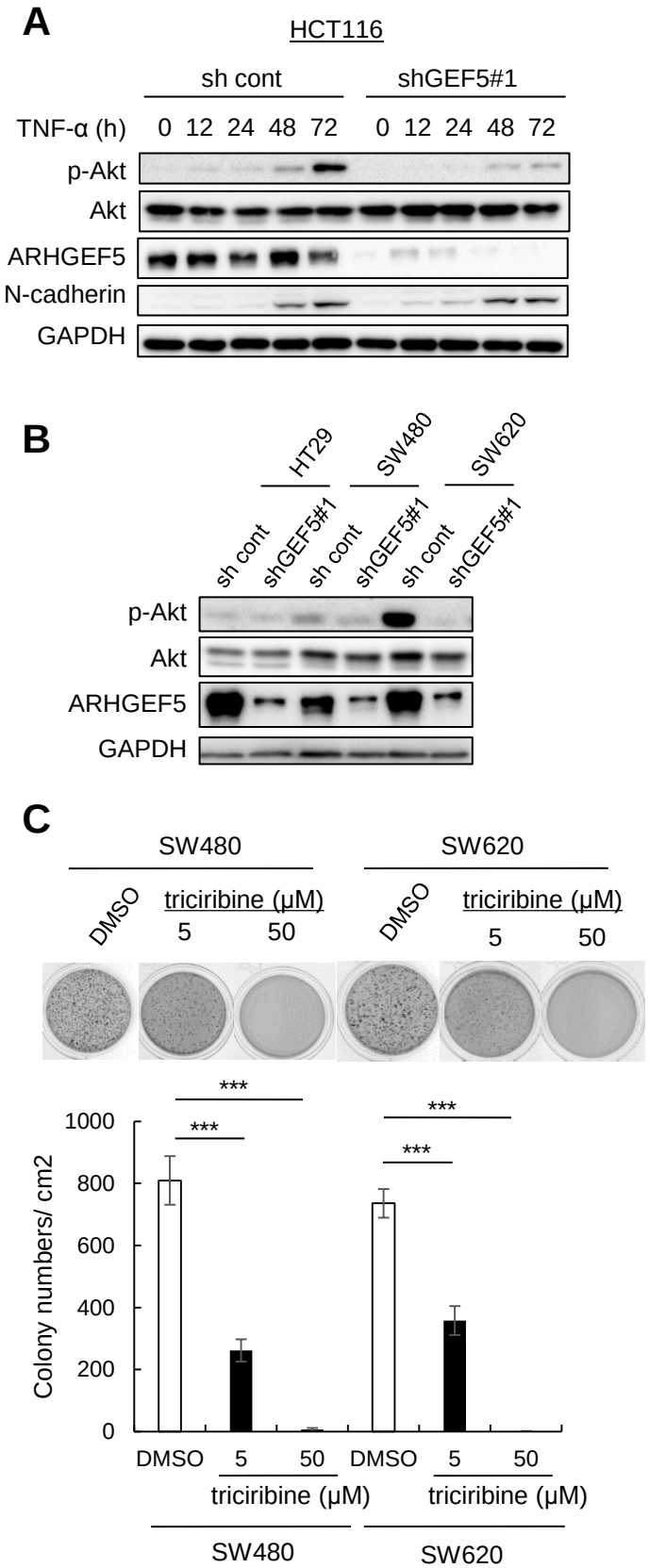
A
HCT116
sh cont
shGEF5#1
TNF-α (h)
0 12 24 48 72
0 12 24 48 72
p-Akt
Akt
ARHGEF5
N-cadherin
GAPDH
B
HT29
SW480
SW620
sh cont
shGEF5#1
sh cont
shGEF5#1
sh cont
shGEF5#1
p-Akt
Akt
ARHGEF5
GAPDH
C
SW480
SW620
DMSO
triciribine (μM)
5
50
DMSO
triciribine (μM)
5
50
***
***
***
***
Colony numbers/ cm2
1000
800
600
400
200
0
DMSO
5
50
DMSO
5
50
triciribine (μM)
triciribine (μM)
SW480
SW620

Fig. 10

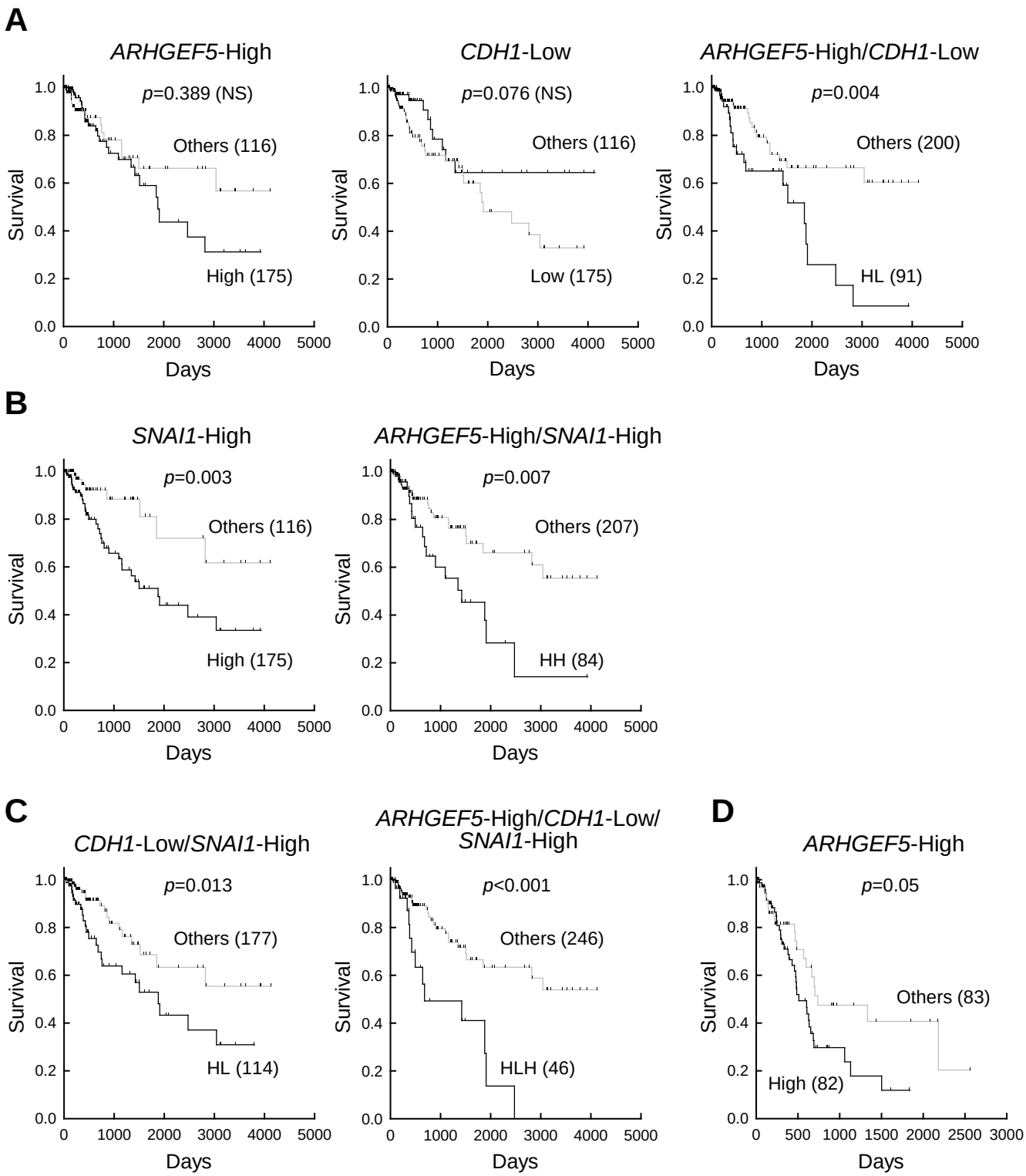
A
ARHGEF5-High
p=0.389 (NS)
Others (116)
High (175)
CDH1-Low
p=0.076 (NS)
Others (116)
Low (175)
ARHGEF5-High/CDH1-Low
p=0.004
Others (200)
HL (91)
B
SNAI1-High
p=0.003
Others (116)
High (175)
ARHGEF5-High/SNAI1-High
p=0.007
Others (207)
HH (84)
C
CDH1-Low/SNAI1-High
p=0.013
Others (177)
HL (114)
ARHGEF5-High/CDH1-Low/
SNAI1-High
p<0.001
Others (246)
HLH (46)
D
ARHGEF5-High
p=0.05
Others (83)
High (82)
Survival
Days

Fig. 11

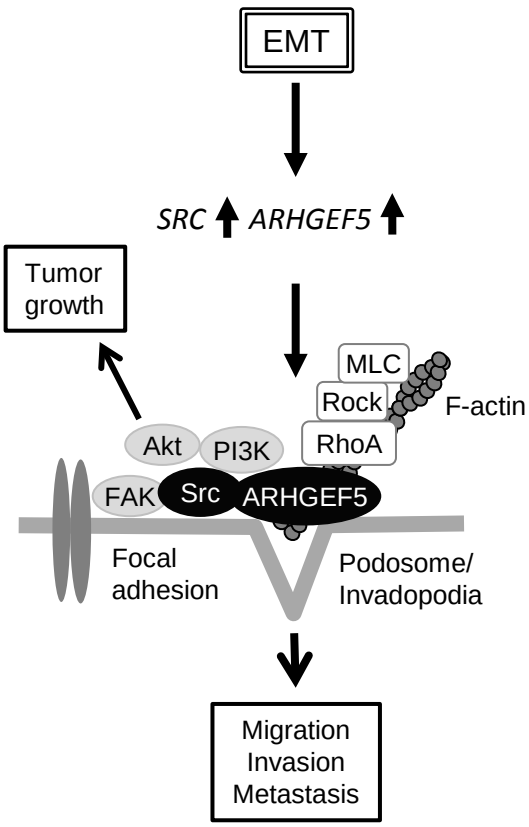
EMT
SRC
ARHGEF5
Tumor growth
MLC
Rock
F-actin
RhoA
Akt
PI3K
FAK
Src
ARHGEF5
Focal adhesion
Podosome/ Invadopodia
Migration
Invasion
Metastasis

Figure legends

Figure 1. EMT is induced by TGF-β in MCF10A cells.

(A) MCF10A cells were treated with or without TGF-β1 for 48 h and stained for E-cadherin, N-cadherin, and F-actin. Cell morphology was observed under a phase-contrast microscope (PC). White arrowheads in the F-actin images indicate the locations of podosome-like structures. Scale bar: 20 μm. (B) MCF10A cells were treated with TGF-β1 for the indicated periods, and the levels of the indicated proteins analyzed by western blotting. (C) MCF10A cells treated with or without TGF-β1 were subjected to wound-healing assays. Scale bar: 100 μm. Values represent the mean ± SD (n=3, **p<0.01).

Figure 2. ARHGEF5 and Src are upregulated during TGF-β-induced EMT in MCF10A cells.

(A) Expression of ARHGEF5 and phospho-MLC in TGF-β1-treated MCF10A cells was analyzed by western blotting. Values represent the mean ± SD (n=3, *p<0.05, ***p<0.001). (B) Expression of ARHGEF5 mRNA in TGF-β1-treated MCF10A cells was assessed by RT-PCR. (C) MCF10A cells were treated with SD208 and the levels of the indicated proteins analyzed by western blotting. (D) Expression of the indicated proteins in TGF-β1-treated MCF10A cells was analyzed by western blotting. (E) MCF10A cells treated with or without TGF-β1 for 48h were immunostained for ARHGEF5. White arrowheads indicate the ARHGEF5 positive areas in lamellipodia. Scale bar: 20 μm.

Figure 3. ARHGEF5 KD attenuates TGF-β-induced EMT and cell migration in MCF10A cells.

(A) ARHGEF5 was knocked down with shRNAs (shGEF5#1 and shGEF5#2) in MCF10A cells. Mock and ARHGEF5-KD cells were treated with or without

TGF-β1 for 24 h and the levels of the indicated proteins analyzed by western blotting. (B) Mock and ARHGEF5 KD cells were treated with or without TGF-β1 for 48 h and the cells stained with anti-N-cadherin or anti-E-cadherin. Scale bar: 20 μm. (C) Mock and ARHGEF5 KD cells were treated with or without TGF-β1 for 24h and subjected to wound-healing assays. Scale bar: 200 μm. (D) The migration rates of the indicated cells are shown. Values represent the mean ± SD (n=3, ***p<0.001)

Figure 4. The ROCK inhibitor, Y27632, suppresses TGF-β-induced EMT phenotypes in MCF10A cells.

(A) MCF10A cells were treated with TGF-β for 48 h in the presence or absence of Y27632 and the cells stained with anti-E-cadherin or anti-N-cadherin. Scale bar: 20 μm. (B) MCF10A cells were treated with TGF-β for 48 h in the presence or absence of Y27632 and then subjected to wound-healing assays.

Scale bar: 200 μm. (C) The migration rates of the indicated cells are shown. Values represent the mean ± SD (n=3, ***p<0.001). (D) MCF10A cells overexpressing Flag-ARHGEF5 were treated with Y27632 for 24h and MLC phosphorylation and the indicated proteins was analyzed by western blotting.

Figure 5. ARHGEF5 KD does not affect expression of EMT-related transcription factors.

Mock and ARHGEF5-KD MCF10A cells were treated with or without TGF-β for the indicated periods and expression of the indicated EMT-related transcription factors was assessed by RT-PCR.

Figure 6. ARHGEF5 KD suppresses the invasive activity of human colorectal cancer HCT116 cells.

(A) ARHGEF5 in HCT116 cells was knocked down with siRNAs (siGEF5#1 and siGEF5#3) in HCT116 cells and downregulation of ARHGEF5 confirmed by western blotting (upper). Control and siRNA-treated HCT116 were stained for F-actin. Scale bar: 20 μm. (B) Control and siRNA-treated HCT116 cells were subjected to an in vitro wound-healing assay. Scale bar: 200 μm. Values represent the mean ± SD (n=3, **p<0.01). (C) The in vitro invasive activity of control HCT116 cells and those treated with specific siRNAs was examined in a Matrigel Transwell assay. Yellow arrowheads indicate invaded cells. Scale bar: 20 μm. Values represent the mean ± SD (n = 3, *p<0.05). (D) The in vivo metastatic activity of HCT116 cells transfected with control and shGEF#1 was examined in experimental metastasis assays in nude mice. Metastatic lesions were observed by staining tissue slices with hematoxylin-eosin. Black arrowheads indicate metastatic lesions. Magnified views of the lesions in mice C4 and C5 are shown.

Figure 7. ARHGEF5 is required for tumor growth in mesenchymal-like cancer cells.

(A) Expression of ARHGEF5 and the indicated EMT marker proteins in the indicated colorectal cancer cells was analyzed by western blotting. (B) ARHGEF5 in the indicated cells was stably knocked down by shRNA and the efficacy confirmed by western blotting. (C) Mock and ARHGEF5-KD HCT116 and HT29 cells were subjected to soft agar colony formation assays. Values represent the mean ± SD (n=3, N.S., not significant). (D) Mock and ARHGEF5-KD SW480 and SW620 cells were subjected to soft agar colony formation assays. Values represent the mean ± SD (n=3, ***p<0.001, *p<0.05). (E) Mock and ARHGEF5 KD SW480 cells were subcutaneously inoculated into nude mice. Tumors generated 1 month after inoculation were

excised and photographed. Tumors obtained from two independent experiments, Exp.1 (n=4) and Exp.2 (n=3), are shown. Scale bar: 2 cm.

Figure 8. ARHGEF5 is required for tumor growth from HCT116 cells that haveundergone EMT.

(A) Mock and ARHGEF5 KD HCT116 cells were treated with TNF-α for 72 h, and expression of the indicated EMT markers was analyzed by western blotting (lower panels). (B) Mock and ARHGEF5 KD HCT116 cells treated with TNF-α were subjected to soft agar colony formation assays. Values represent the mean ± SD (n=3, ***p<0.001). (C) Mock and ARHGEF5-KD HCT116 cells were stably transfected with or without myc-tagged Slug, and cell morphology observed (upper). Scale bar: 100 μm. The levels of the indicated EMT markers were analyzed by western blotting (lower). (E) HCT116 cells transfected with the indicated constructs were subjected to soft agar colony formation assays. Values represent the mean ± SD (n=3, *p<0.05).

Figure 9. ARHGEF5-dependent activation of Akt is required for tumor growth from mesenchymal-like colorectal cancer cells.

(A) HCT116 cells were treated with TNF-α (50 ng/ml) for the indicated periods, and the levels of the indicated proteins analyzed by western blotting. (B) HT29, SW480, and SW620 cells were transfected with control shRNA or shGEF5#1 and the levels of the indicated proteins analyzed by western blotting. (C) SW480 and SW620 cells treated with DMSO or with the indicated concentrations of Akt inhibitor were subjected to soft-agar colony formation assays. Values represent the mean ± SD (n=3, ***p<0.001).

Figure 10. ARHGEF5 upregulation associated with EMT-related gene expression correlates with poor prognosis in patients with colorectal cancers.

The correlation between ARHGEF5 and E-cadherin (CDH1) (A), ARHGEF5 and Snail (SNAI1) (B), and ARHGEF5, CDH1, and SNAI1 (C) expression and prognosis in colorectal cancer patients was estimated using the Kaplan-Meier method42 based on the transcriptome dataset from the TCGA project. Statistical significance was calculated using the log rank test. (D) The correlation between ARHGEF5 expression and the prognosis of pancreatic cancer patients was estimated.

Figure 11. Model of Arhgef5 functions.

Materials and methods

Reagents and antibodies

Anti-ARHGEF5 was generated in rabbits via immunization with GST-mouse or human ARHGEF5 (aa 2-204) and affinity purified using a maltose-binding protein-tagged antigen. Anti-Src-pY418, anti-GFP, anti-FAK-pY397, SD208, Alexa Fluor 488 phalloidin, Alexa Fluor 594-conjugated goat anti-rabbit IgG, HRP-conjugated goat anti-rabbit IgG, anti-mouse IgG, anti-occludin, and anti-cortactin-pY421 were purchased from Thermo Fisher Scientific (Waltham, MA, USA). Anti-GAPDH, anti-Fyn, anti-Lyn, and anti-vimentin were from Santa Cruze Biotechnology (Santa Cruz, CA, USA). Anti-v-Src, anti-cortactin (4F11) and anti-phosphotyrosine (4G10) were from Millipore (Billerica, MA, USA). Anti-FLAG (M2) and anti-β-tubulin were from Sigma-Aldrich (St Louis, MO, USA). Anti-E-cadherin, anti-N-cadherin, and anti-FAK were from BD Transduction Laboratories (Lexington, KY, USA). Anti-Smad2-pS465/467, anti-Smad2, anti-MLC2-pT18/S19, anti-MLC2, anti-Akt and anti-Akt-pS473 were from Cell Signaling Technology Inc. (Beverly, MA, USA). TGF-β1 and TNF-α were from PeproTech (Rocky Hill,

NJ, USA). The Akt inhibitor triciribine was from Selleckchem (Houston, TX, USA)

Cell culture

The normal breast epithelial cell line MCF10A and the human colon cancer cell lines Caco-2, SW480, SW620, HCT116, and HT29 were purchased from the American Type Culture Collection (Manassas, VA, USA). ARHGEF5 KO cells were established by transfecting ARHGEF5fl/fl MEFs with a Cre vector (gifted by Dr. Masahito Ikawa, Osaka University, Japan). All cells were cultured at 37°C in a humidified atmosphere containing 5% CO2. MCF10A cells were maintained in Dulbecco's Modified Eagle's Medium (DMEM) supplemented with 5% horse serum, Ham's F12 Nutrient Mixture (Thermo Fisher Scientific), 20ng/ml EGF, 100ng/ml cholera toxin, 500ng/ml hydrocortisone and 5μg/ml insulin. SW480, SW620, HCT116 and HT29 cells were maintained in DMEM supplemented with 10% (v/v) fetal bovine serum (FBS) and penicillin/streptomycin.

Plasmid and siRNA constructs

ARHGEF5 cDNA with a 3xFLAG tag was subcloned into the pCX4-bsr vector (gifted by Dr. Tsuyoshi Akagi, KAN Research Institute, Kobe, Japan). ARHGEF5 GFP, ARHGEF5 ΔDH (deleted amino acids, 1158-1341) and ARHGEF5 were subcloned into the pCX4-bsr vector. Myc-tagged Snail and Slug cDNAs were subcloned into the pCX4-bleo vector. Lentiviral vectors carrying sh-ARHGEF5#1 (shGEF5#1) and sh-ARHGEF5#2 (shGEF5#2) were

purchased from Sigma-Aldrich. The series of ARHGEF5 siRNA duplexes (siGEF5#1-3) (Stealth, MSS225557) and Stealth siRNA Negative Control (12935-112) were purchased from Invitrogen (Carisbad, CA, USA). The

sequences of shRNAs and siRNAs are as follows:

shGEF5#1,

5’-CCGGGCAACATGACAAACTTCCTATCTCGAGATAGGAAGTTTGTCATG TTGCTTTTT-3’;

shGEF5#2,

5’-CCGGCTCTCAAGAATCCATCTCAAACTCGAGTTTGAGATGGATTCTTG AGAGTTTTT-3’;

siGEF5#1,

5’-UUCAGAGGAAGGAUCUAUGAUAGGGCCCUAUCAUAGAUCCUUCCU CUGAA-3’;

siGEF5#2,

5’-UAAGCAGUUCACUUCCACUGCCCUGCAGGGCAGUGGAAGUGAACU GCUUA-3’;

and siGEF5#3,

5’-UGUAUUAUUAAAUUCCUCCUGAGGGCCCUCAGGAGGAAUUUAAU AAUACA-3’.

RT-PCR and primers

Total RNA was prepared using Sepazol Super G (Nacalai tesque, Kyoto, Japan). Reverse transcription was carried out using the Transcriptor First Strand cDNA Synthesis Kit (Roche, Basel, Switzerland). PCR was performed using the following primers.

ARHGEF5 forward, 5’-CAGTCCTGCTGAAGCCTACC-3’;

ARHGEF5 reverse, 5’-GGGAACCACTACACGAGCAT-3’;

GAPDH forward, 5’-CGAGATCCCTCCAAAATCAA-3’;

GAPDH reverse, 5’-TGCTGTAGCCAAATTCGTTG-3’;

ACTA2 forward, 5'-TTCAATGTCCCAGCCATGTA-3';

ACTA2 reverse, 5'-GAAGGAATAGCCACGCTCAG-3';

SNAI1 forward, 5'-TTTACCTTCCAGCAGCCCTA-3';

SNAI1 reverse, 5'-CCCACTGTCCTCATCTGACA-3';

SNAI2 forward, 5'-TCGGACCCACACATTACCTT-3';

SNAI2 reverse, 5'-TTGGAGCAGTTTTTGCACTG-3';

SNAI3 forward, 5'-ACTGCCACAAACCCTACCAC-3';

SNAI3 reverse, 5'-ATAGGGCTTCTCCCCTGTGT-3';

TWIST1 forward, 5'-GTCCGCAGTCTTACGAGGAG-3';

TWIST1 reverse, 5'-TGGAGGACCTGGTAGAGGAA-3';

TWIST2 forward, 5'-AGCAAGAAGTCGAGCGAAGA-3';

TWIST2 reverse, 5'-CAGCTTGAGCGTCTGGATCT-3';

ZEB1 forward, 5'-TGCACTGAGTGTGGAAAAGC-3';

ZEB1 reverse, 5'-TGGTGATGCTGAAAGAGACG-3';

ZEB2 forward, 5'-CGCTTGACATCACTGAAGGA-3'; and

ZEB2 reverse, 5'-CTTGCCACACTCTGTGCATT-3'.

Transfection

Retroviral and lentiviral gene transfer, and lipofection Gene-transfer experiments were performed using the pCX4 series of retroviral vectors[41]. pCX4 vectors were transfected into PLT cells using FuGENE (Roche) and the culture supernatant used as the source of virus. KD of ARHGEF5 was performed using lentiviral vectors. Lentiviruses were generated from PLT cells using the MISSION Lentiviral packaging mix (Sigma-Aldrich) and FuGENE. siRNA and cDNA were transiently transfected using RNAimax and Lipofectamine 3000 (Thermo Fisher Scientific), respectively. The active form of Src (SrcF572) was introduced into MEFs and MCF10A cells using the Retro-X Tet-On 3G Inducible Expression System (Clontech, Mountain view,

CA, USA).

Western blotting

Cells were lysed in SDS-sample buffer (2% SDS, 62.5 mM Tris-HCl [pH 6.8], 5% sucrose). Equal amounts of total proteins were separated by SDS-PAGE and transferred onto polyvinylidene difluoride (PVDF) membranes. Membranes were blocked and incubated with primary antibodies, followed by incubation with HRP-conjugated secondary antibodies. Signals were visualized on a WSE6200H luminograph II (ATTO, Tokyo, Japan). Representative blots obtained from at least three independent experiments are shown.

Soft agar colony formation assay

DMEM (1.25 ml) supplemented with 10% FBS and 0.7% Bacto-Agar (BD Transduction Laboratories) was placed in each well of a 12-well plate (bottom layer). After the agar solidified, cells (in 1 ml of culture medium + 0.36% agar) were poured onto the bottom layer. After 5–14 days, colonies were fixed and stained with 1 mg/ml 3-(4,5-dimethylthiazol-2-yl)-2,5-diphenyltetrazolium bromide (MTT). Colonies were counted using ImageJ.

Immunohistochemistry

Cells were seeded on a 12 mm coverslip coated with 5 μg/ml fibronectin. The samples were fixed in 4% paraformaldehyde (PFA), and permeabilized with 0.1% Triton-X in PBS (T-PBS). Samples were blocked with 1% BSA in T-PBS, and then incubated with primary antibody overnight at 4°C, followed by incubation with secondary antibody at room temperature. After the samples were washed with T-PBS, coverslips were mounted on glass slides using ProLong Gold (Thermo Fisher Scientific). The next day, the coverslips were

sealed with ProLong Gold Antifade reagent and observed under a confocal microscope (FV1000, OLYMPUS, Tokyo, Japan). The same experiments were repeated at least three times.

Invasion assay

BioCoat Matrigel Invasion Chambers (BD Biosciences) were used for the invasion assay. Cells (5×10^4 for HCT116) were seeded on inserts and moved into chambers containing culture supernatant of NIH3T3 cells. After incubation at 37°C for 48 h, invaded cells were fixed with 100% methanol and then stained with 0.1% toluidine blue. Invaded cells were counted on micrographs; in each experiment, cells were counted on five randomly chosen fields. Experiments were repeated at least three times.

In vivo metastasis assay

HCT116 cells transfected with or without ARHGEF5 shRNA (3×10^6 in 100 µl of serum-free medium) were intravenously injected into six nude mice (BALB/c Slc-nu/nu, 4 weeks old, female). After 7 weeks, the surviving mice were sacrificed and their lungs removed. Metastatic lesions were detected by staining the tissue slices with hematoxylin-eosin in a blind test. Mice were handled and maintained according to the Osaka University guidelines for animal experimentation.

In vivo tumorigenicity assay

SW480 cells transfected with or without ARHGEF5 shRNAs (4×10^6 in 200 µl of serum-free medium) were subcutaneously injected into nude mice (BALB/c Slc-nu/nu, 4 weeks old, female). After 2-4 weeks, the surviving mice were sacrificed, their tumors were removed, and the sizes and weight of the tumors were measured. Mice were handled and maintained according to the Osaka University guidelines for animal experimentation.

Kaplan-Meier survival analysis

Clinical and RNA-seq data from the publically available TCGA dataset from 291 colon adenocarcinoma or 165 pancreatic adenocarcinoma patients were used for analysis of ARHGEF5, E-cadherin and Snail expression in tumor samples. Survival curves were estimated using the Kaplan-Meier method, and the obtained survival curves were compared by using the log rank test.

References

1. Valastyan S, Weinberg RA. Tumor metastasis: molecular insights and evolving paradigms. Cell 2011; 147: 275-292.

2. Hanahan D, Weinberg RA. Hallmarks of cancer: the next generation. Cell 2011; 144: 646-674.

3. Lamouille S, Xu J, Derynck R. Molecular mechanisms of epithelial-mesenchymal transition. Nat Rev Mol Cell Biol 2014; 15: 178-196.

4. Bill R, Christofori G. The relevance of EMT in breast cancer metastasis: Correlation or causality? FEBS Lett 2015; 589: 1577-1587.

5. Kang Y, Massague J. Epithelial-mesenchymal transitions: twist in development and metastasis. Cell 2004; 118: 277-279.

6. Kalluri R, Weinberg RA. The basics of epithelial-mesenchymal transition. J Clin Invest 2009; 119: 1420-1428.

7. Miyazono K. Transforming growth factor-beta signaling in epithelial-mesenchymal transition and progression of cancer. Proc Jpn Acad Ser B Phys Biol Sci 2009; 85: 314-323.

8. Mikami S, Mizuno R, Kosaka T, Saya H, Oya M, Okada Y. Expression of TNF-alpha and CD44 is implicated in poor prognosis, cancer cell invasion,

metastasis and resistance to the sunitinib treatment in clear cell renal cell carcinomas. Int J Cancer 2015; 136: 1504-1514.

9. Wu ST, Sun GH, Hsu CY, Huang CS, Wu YH, Wang HH et al. Tumor necrosis factor-alpha induces epithelial-mesenchymal transition of renal cell carcinoma cells via a nuclear factor kappa B-independent mechanism. Exp Biol Med (Maywood) 2011; 236: 1022-1029.

10. Vergara D, Merlot B, Lucot JP, Collinet P, Vinatier D, Fournier I et al. Epithelial-mesenchymal transition in ovarian cancer. Cancer Lett 2010; 291: 59-66.

11. Tam WL, Weinberg RA. The epigenetics of epithelial-mesenchymal plasticity in cancer. Nat Med 2013; 19: 1438-1449.

12. Samatov TR, Tonevitsky AG, Schumacher U. Epithelial-mesenchymal transition: focus on metastatic cascade, alternative splicing, non-coding RNAs and modulating compounds. Mol Cancer 2013; 12: 107.

13. Kyprianou N. ASK-ing EMT not to spread cancer. Proc Natl Acad Sci U S A 2010; 107: 2731-2732.

14. Peinado H, Olmeda D, Cano A. Snail, Zeb and bHLH factors in tumour progression: an alliance against the epithelial phenotype? Nat Rev Cancer 2007; 7: 415-428.

15. Neel DS, Bivona TG. Secrets of drug resistance in NSCLC exposed by new molecular definition of EMT. Clin Cancer Res 2013; 19: 3-5.

16. Voulgari A, Pintzas A. Epithelial-mesenchymal transition in cancer metastasis: mechanisms, markers and strategies to overcome drug resistance in the clinic. Biochim Biophys Acta 2009; 1796: 75-90.

17. Brown MT, Cooper JA. Regulation, substrates and functions of src. Biochim Biophys Acta 1996; 1287: 121-149.

18. Yeatman TJ. A renaissance for SRC. Nat Rev Cancer 2004; 4: 470-480.

19. Frame MC. Newest findings on the oldest oncogene; how activated src does it. J Cell Sci 2004; 117: 989-998.

20. Silva CM. Role of STATs as downstream signal transducers in Src family kinase-mediated tumorigenesis. Oncogene 2004; 23: 8017-8023.

21. Kuroiwa M, Oneyama C, Nada S, Okada M. The guanine nucleotide exchange factor Arhgef5 plays crucial roles in Src-induced podosome formation. J Cell Sci 2011; 124: 1726-1738.

22. Linder S, Aepfelbacher M. Podosomes: adhesion hot-spots of invasive cells. Trends Cell Biol 2003; 13: 376-385.

23. Saykali BA, El-Sibai M. Invadopodia, regulation, and assembly in cancer cell invasion. Cell Commun Adhes 2014; 21: 207-212.

24. Yohe ME, Rossman KL, Gardner OS, Karnoub AE, Snyder JT, Gershburg S et al. Auto-inhibition of the Dbl family protein Tim by an N-terminal helical motif. J Biol Chem 2007; 282: 13813-13823.

25. Narumiya S, Tanji M, Ishizaki T. Rho signaling, ROCK and mDia1, in transformation, metastasis and invasion. Cancer Metastasis Rev 2009; 28: 65-76. 26. Mihira H, Suzuki HI, Akatsu Y, Yoshimatsu Y, Igarashi T, Miyazono K et al. TGF-beta-induced mesenchymal transition of MS-1 endothelial cells requires Smad-dependent cooperative activation of Rho signals and MRTF-A. J Biochem 2012; 151: 145-156.

27. Wang Z, Kumamoto Y, Wang P, Gan X, Lehmann D, Smrcka AV et al. Regulation of immature dendritic cell migration by RhoA guanine nucleotide exchange factor Arhgef5. J Biol Chem 2009; 284: 28599-28606.

28. Takai S, Chan AM, Yamada K, Miki T. Assignment of the human TIM proto-oncogene to 7q33-->q35. Cancer Genet Cytogenet 1995; 83: 87-89.

29. Chan AM, McGovern ES, Catalano G, Fleming TP, Miki T. Expression cDNA cloning of a novel oncogene with sequence similarity to regulators of small GTP-binding proteins. Oncogene 1994; 9: 1057-1063.

30. He P, Wu W, Yang K, Tan D, Tang M, Liu H et al. Rho Guanine Nucleotide Exchange Factor 5 Increases Lung Cancer Cell Tumorigenesis via MMP-2 and Cyclin D1 Upregulation. Mol Cancer Ther 2015; 14: 1671-1679.

31. He P, Wu W, Wang H, Liao K, Zhang W, Xiong G et al. Co-expression of Rho guanine nucleotide exchange factor 5 and Src associates with poor prognosis of patients with resected non-small cell lung cancer. Oncol Rep 2013; 30: 2864-2870.

32. Yang L, Yang J, Venkateswarlu S, Ko T, Brattain MG. Autocrine TGFbeta signaling mediates vitamin D3 analog-induced growth inhibition in breast cells. J Cell Physiol 2001; 188: 383-393.

33. Timpson P, Jones GE, Frame MC, Brunton VG. Coordination of cell polarization and migration by the Rho family GTPases requires Src tyrosine kinase activity. Curr Biol 2001; 11: 1836-1846.

34. Shih JY, Yang PC. The EMT regulator slug and lung carcinogenesis. Carcinogenesis 2011; 32: 1299-1304.

35. Cancer Genome Atlas Research N. Integrated genomic analyses of ovarian carcinoma. Nature 2011; 474: 609-615.

36. Masszi A, Di Ciano C, Sirokmany G, Arthur WT, Rotstein OD, Wang J et al. Central role for Rho in TGF-beta1-induced alpha-smooth muscle actin expression during epithelial-mesenchymal transition. Am J Physiol Renal Physiol 2003; 284: F911-924.

37. Spinardi L, Marchisio PC. Podosomes as smart regulators of cellular adhesion. Eur J Cell Biol 2006; 85: 191-194.

38. Berdeaux RL, Diaz B, Kim L, Martin GS. Active Rho is localized to podosomes induced by oncogenic Src and is required for their assembly and function. J Cell Biol 2004; 166: 317-323.

39. Bar-Peled L, Sabatini DM. SnapShot: mTORC1 signaling at the lysosomal surface. Cell 2012; 151: 1390-1390 e1391.

40. Cheung KJ, Gabrielson E, Werb Z, Ewald AJ. Collective invasion in breast cancer requires a conserved basal epithelial program. Cell 2013; 155: 1639-1651.

41. Akagi T, Sasai K, Hanafusa H. Refractory nature of normal human diploid fibroblasts with respect to oncogene-mediated transformation. Proc Natl Acad Sci U S A 2003; 100: 13567-13572.

42. Kaplan EL, Meier P. Nonparametric-Estimation from Incomplete Observations. J Am Stat Assoc 1958; 53: 457-481.

References of general introduction

1, World health organization. Latest world cancer statistics Global cancer burden rises to 14.1 million new cases in 2012. International agency for research on cancer. 2013.

2, Douglas Hanahan and Robert A. Weinberg. Hallmarks of Cancer. Cell. 2000; 100: 57–70.

3, Douglas Hanahan and Robert A. Weinberg. Hallmarks of Cancer: The Next Generation. Cell. 2011; 144, 5: 646-674.

4, Masato Okada. Regulation of the Src Family Kinases by Csk. Int J Biol Sci. 2012; 8(10):1385-1397.

5, Complex networks orchestrate epithelial–mesenchymal transitions. Jean Paul Thiery and Jonathan P. Sleeman. Nature Reviews Molecular Cell

Biology. 2006; 7, 131-142.

6, Epithelial-Mesenchymal Transitions in Development and Disease. Jean Paul Thiery, Hervé Acloque, Ruby Y.J. Huang, M. and Angela Nieto. Cell. 2009; 139, 5:871–890.

Publication

The Rho guanine nucleotide exchange factor ARHGEF5 promotes tumor malignancy via epithelial-mesenchymal transition

Accepted on 20th July in *Oncogenesis*

Yu Komiya, Yasuhito Onodera, Miho Kuroiwa, Suguru Nomimura, Yuki Kubo, Jin-Min Nam, Kentaro Kajiwara, Shigeyuki Nada, Chitose Oneyama, Hisataka Sabe, and Masato Okada

Acknowledgments

We thank T. Akagi for the generous gift of the modified pCX4 vector, M. Ikawa for the integrase-defective Cre vector, Y. Kurahashi and H. Nishida for technical assistance, and J-J. Choo, W-Y. Chee and R. Matsuyama for critical reading of the manuscript. This work was supported by JSPS KAKENHI Grant Numbers 15H04296, 26640078, and 26114006.